Near-field microwave microscope measurements to characterize bulk material properties

Atif Imtiaz,[a] Thomas Baldwin, Hans T. Nembach, Thomas M. Wallis, and Pavel Kabos
National Institute of Standards and Technology, Boulder, Colorado 80305

(Received 2 April 2007; accepted 18 May 2007; published online 12 June 2007)

The authors discuss near-field scanning microwave microscope measurements of the complex permittivity for bulk dielectric (fused silica), semiconductor (silicon), and metal (copper). The authors use these measurements to test existing quasistatic theoretical approach to deembed the bulk material properties from the measured data. The known quasistatic models fit the measured data well with parameters for silicon (ε_s=11.9, σ_{Si}=50 S/m) and fused silica (ε_s=3.85, tan δ=1.0×10^{-4}). However, for copper (with $\sigma_{Cu}=5.67\times10^7$ S/m), apart from quasistatic coupling, an additional loss of 12 Ω is needed to fit the data. © *2007 American Institute of Physics*. [DOI: 10.1063/1.2748307]

High frequency nanoscale devices enable innovative technologies but often require integration of semiconductors, dielectrics, and metals into nanometer-scale devices. This trend is evident in the device structures coming from scaling of transistor-based electronics down to 32 nm (Refs. 1 and 2) as well as emerging nanotube-based and spintronic devices.[2–5] Such applications require tools for measurement of material properties on nanometer length scales at high frequencies.[1] One tool for characterization of composite nanoscale materials at microwave frequencies is the near-field scanning microwave microscope (NSMM).[6–13] Two major trends in NSMM are a waveguide approach[9] and a sharp-tip approach.[8,10–13] For studying nanodevices, the sharp-tip approach of NSMM has several advantages, including the use of scanning tunneling microscopy (STM) feedback as a distance-following mechanism for NSMM.[12] With STM-assisted NSMM, nanoscale spatial resolution has been achieved in capacitance[12] and sheet resistance.[14] However, the physics of a sharp tip in the near-field is still not completely understood,[7] despite the fact that NSMM has been used for nanoscale measurements. In this letter, we extend the conventional antenna theory to better understand the interaction of the sharp tip with materials as it is brought into the near field of different bulk samples.

The bulk samples are used to simplify the sample geometry, since NSMM is sensitive to material properties as well as the geometry of the tip and sample.[7] One of the challenges in this field is to deembed the material properties of the sample from geometrical effects.[6,7] We performed height-dependent NSMM measurements over semiconducting, dielectric, and metal samples in order to understand the physics related to the sharp-tip geometry and tip-sample interaction. Below, we show that a loss mechanism due to the sharp tip becomes a significant factor in the characterization of high conductivity materials. We also discuss a way to qualify bulk materials based on the magnitude of their respective complex permittivities.

To perform measurements, we employed a commercially available NSMM system described in detail elsewhere.[8] The critical part of the NSMM system is a λ/4 coaxial resonator operating at 2.66 GHz with an aperture opening and a sharp tip sticking out at one end, as shown in Fig. 1. The resonator is connected to a vector network analyzer through input and output coupling loops. The measurement is performed in transmission mode by measuring the S_{12} or S_{21} scattering matrix parameters of the resonator. The resonant frequency (f) and quality factor (Q) are measured as a function of the height of the tip above the sample (z). We define f_0 and Q_0 the resonant frequency and quality factor of the resonator with no sample present ($z\geqslant1$ mm). The Q_0 of the resonator is 652. The frequency shift is defined as $\Delta f=f-f_0$. The zero height is defined as the point where the tip touches the sample. In the experiment, we changed the height by moving away from the sample starting at the touching point. Note that the minimum step size of z is 0.1 μm.

To analyze the experimental data, we used a series-*RLC* lumped element model for the resonator. Following the approach introduced in Ref. 11, the sample load is electrically in parallel with the capacitance of the resonator. Figure 1 shows the experimental setup with the defined lumped elements. The tip-to-sample coupling capacitance C_c consists of two capacitors in series: the tip-to-sample geometrical capacitance (C_x) and the material capacitance (C_s).[15] The capacitance between the outer conductor of the resonator and the bulk sample (C_{out}) can be safely ignored, since $C_{out}\gg C_c$. In our analysis, C_x is modeled with the quasistatic imaging methods,[8] and the loading impedance of the sample is modeled as a series capacitor C_s and sample resistance R_s.[7] As discussed below, the analysis of experimental data shows

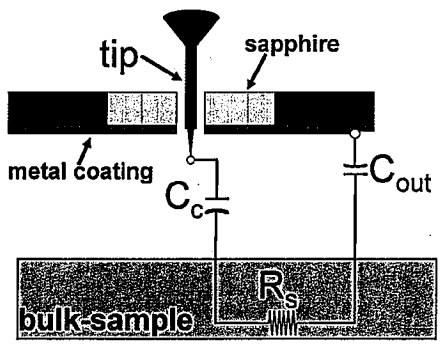

FIG. 1. Experimental setup of NSMM. The tip is the antenna brought near the sample. The coupling capacitance C_c is in series with the materials' property R_s. C_c has contributions from both the sample material and the tip-sample geometry.

[a]Electronic mail: atif@boulder.nist.gov

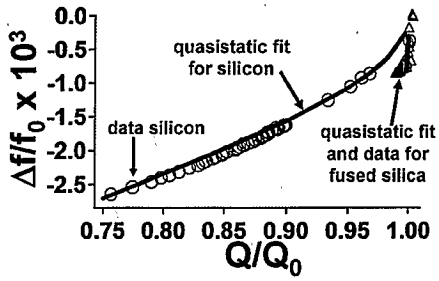

FIG. 2. (Color online) $\Delta f/f_0$ vs Q/Q_0 plotted for the silicon and fused silica. The y axis is sensitive to C_c to first order, and the x axis to the materials' loss. Both materials fit well with the conventional quasistatic models. The measurement was performed at heights from 0.1 to 1000 μm.

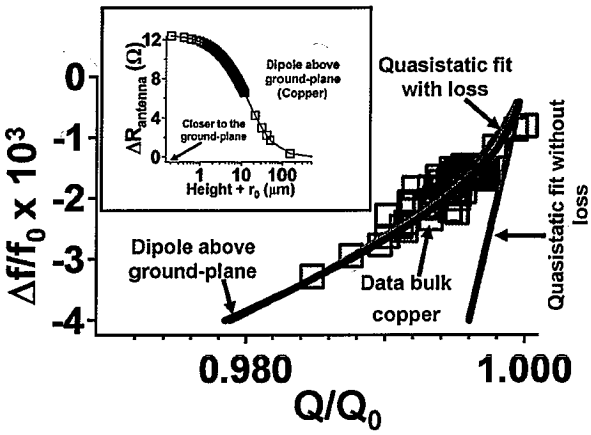

FIG. 3. (Color online) $\Delta f/f_0$ vs Q/Q_0 for copper. The data (open squares) require additional loss of 12 Ω in addition to conventional quasistatic models. The inset shows the 12 Ω loss originating from the Hertzian vertical electric dipole being brought close to the conducting ground plane.

that Δf is sensitive mainly to C_x and C_s while Q is sensitive mainly to R_s. The inductance L_s becomes important for superconducting samples.[7]

The data for the bulk dielectric (fused silica) and bulk semiconductor (silicon) are shown in Fig. 2, where $\Delta f/f_0$ is plotted against Q/Q_0 at each height and this height range is from 0.1 to 1000 μm. The higher the material loss, the lower will be the value of Q/Q_0. To compare our experimental results with the existing material characterization procedures, we used the commonly used fitting parameters in the model: Dr_0 (the effective radius of the antenna wire),[7,9,16] the relative permittivity ε_s, and the conductivity σ of the material. The diameter of the original tungsten wire used as the tip is 80 μm; however, the probe end of the tip was cut, so r_0 is expected to be less than 40 μm. The tip-to-sample static field structure depends on the sample material properties; hence the effective radius of the antenna wire will be different for different materials. We kept r_0 fixed at 30 μm throughout the analysis and varied D to account for the changes in the field structure.

The quasistatic model of tip-sample interaction uses an image-charge method above the bulk dielectric and metal[8] to calculate C_x. Fits using this model are shown as solid lines in Fig. 2. For silicon, the fit parameter is $D=1.35$, with $\sigma_{Si}=50$ S/m ($\rho_{Si}=2$ Ω cm) and $\varepsilon_s=11.9$ held fixed. The quasistatic model fits the silicon data reasonably well. For fused silica, the quasistatic model fits the measured data also reasonably well, but for a different fit parameter $D=2.25$ from the silicon, with fixed $\varepsilon_s=3.85$ and $\tan\delta=1.0\times10^{-4}$, as obtained from independent measurements.[17] The data for the copper are shown in Fig. 3. For the quasistatic fits, the fitting parameters are $D=1$ and $\sigma_{Cu}=5.67\times10^7$ S/m, the conductivity of copper.[18] As shown in Fig. 3, the pure quasistatic model fails to fit the copper data. However, if an additional loss of 12 Ω of resistance is added, then the quasistatic model fits the copper data for the same material parameters.

We attribute this additional 12 Ω of loss to the change of the antenna impedance as it is brought into the near field above the conducting ground plane.[19,20] The inset of Fig. 3 shows the calculation of the change of the real part of the impedance of a Hertzian vertical electric dipole (VED) being brought to the proximity with a semi-infinite conducting ground plane[19,20] with $\sigma=\sigma_{Cu}$. The x axis represents the height plus r_0 of the VED above the ground plane. Here, r_0 represents the location of the center of the VED inside the tip. The change in resistance of the antenna ($\Delta R_{antenna}$) saturates near 12 Ω as the dipole comes closer to the ground plane (copper). The VED fits the copper data for $D=1$, $r_0=30$ μm, with $\sigma=5.67\times10^7$ S/m, and the effective length of the antenna ($L_{ant}=4.6$ mm) as an additional fitting parameter. L_{ant} is larger compared to the actual length of the protruding tip, which is 1.2 mm due to the metal coating on the resonator (shown in Fig. 1) and the ground plane (copper).[21] The presence of the metal coating on the resonator makes the effective antenna length twice the actual length due to the presence of the antenna image.[21] Hence, in the presence of the ground plane (metal), we expect L_{ant} to be four times the actual length. This loss of 12 Ω is significant only for high conductivity materials and becomes insignificant as σ falls below 10^3 S/m,[20] as is the case with silicon. The breakdown of quasistatic approximations is also seen in dielectric thin films above 10 GHz.[22]

It turns out that the magnitude of the complex permittivity can also be used to distinguish between the properties of different bulk materials. When modeled as a series-*RLC* circuit, the input impedance of the resonator is $Z_{in}=R_{resonator}(1+2j(Q\Delta f/f_0))$.[23] Different materials with different complex permittivity values present different loads to the resonator. As a result, the data plotted as the product of Q and Δf should distinguish the materials reflecting the magnitude of their complex permittivity. Figure 4 shows $(\Delta f/f_0)(Q/Q_0)$ for all the studied bulk materials plotted as a function of height. Copper shows the biggest change in the product $(\Delta f/f_0)(Q/Q_0)$, because it has the highest magnitude of complex permittivity, while the fused silica shows the lowest change, because it has the lowest magnitude of complex permittivity.

In contrast, the inset to Fig. 4 shows that by plotting the Q of these materials as a function of height, we cannot distinguish between copper and fused silica. However, the same data plotted in the form of the mentioned product $(\Delta f/f_0)(Q/Q_0)$ as a function of height distinguish all the materials clearly. The fits to the data shown use the same fit parameters as discussed in connection with Fig. 2 for silicon and fused silica and Fig. 3 for copper where the change in the impedance $\Delta Z_{antenna}$ with height has been taken into account. We also note that $(\Delta f/f_0)(Q/Q_0)$ versus height is a capacitance-sensitive way of looking at the data as compared to Δf versus Q, which is loss sensitive. An important goal for the future is to quantitatively understand the capacitance sensitivity of $(\Delta f/f_0)(Q/Q_0)$ for the metals in the region, when

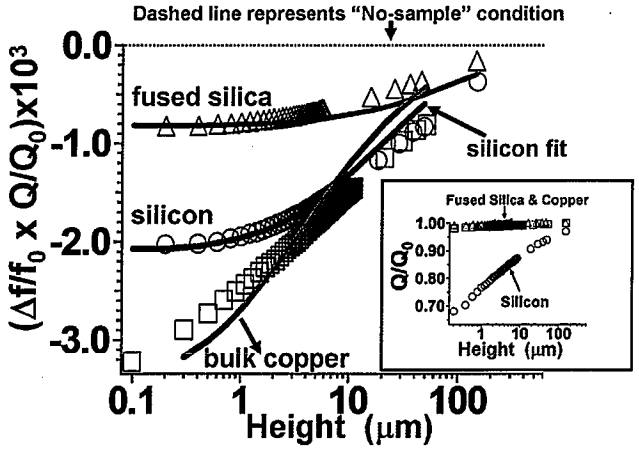

FIG. 4. (Color online) Product $(\Delta f/f_0)(Q/Q_0)$ plotted as a function of height. The copper (complex permittivity magnitude=3.83×10^8) has the biggest variation, while fused silica (complex permittivity magnitude =3.85) has the smallest variation. The inset shows how the same data plotted as Q/Q_0 vs height makes no such clear distinction between the two materials.

the probe-to-sample separation increases (see Fig. 4 for metal).

To conclude, we report on testing of widely used quasistatic deembedding[8] procedures for characterizing the properties of bulk materials with a NSMM sharp tip. An additional loss mechanism due to the change of the antenna impedance coming into the near field above the conducting ground plane[19,20] has to be taken into account to correctly characterize conducting materials. This loss depends on the conductivity of the material and it becomes significant for materials with σ well above 10^3 S/m.[20] For silicon and fused silica, we find quasistatic models to be reasonably sufficient, because for conductivities less than 10^3 S/m,[20] the impedance change due to proximity of the plane boundary with materials can be neglected. Additionally, we introduced a way to distinguish materials with NSMM through the magnitude of the complex permittivity by plotting the product $(\Delta f/f_0)(Q/Q_0)$ as a function of the tip height. The next step is to extend this work to deembedding material properties of more complex, hybrid structures and nanometer-scale devices.

One of the authors (H.T.N) was supported by a fellowship within the Postdoc-Programme of the German Academic Exchange Service (DAAD). The authors would like to thank Steven M. Anlage of the University of Maryland for helpful discussions.

[1]Semiconductor Industry Association, International Technology Roadmap for Semiconductors, 2004, http://www.itrs.net/
[2]H.-S. P. Wong, IBM J. Res. Dev. **46**, 133 (2006).
[3]A. Bachtold, P. Hadley, T. Nakanishi, and C. Dekker, Science **294**, 1317 (2001).
[4]S. Kaka, M. R. Pufall, W. H. Rippard, T. J. Silva, S. E. Russek, and J. A. Katine, Nature (London) **437**, 389 (2005).
[5]F. B. Mancoff, N. D. Rizzo, B. N. Engel, and S. Tehrani, Nature (London) **437**, 393 (2005).
[6]B. T. Rosner and D. W. van der Weide, Rev. Sci. Instrum. **73**, 2505 (2002).
[7]S. M. Anlage, V. V. Talanov, and A. R. Schwartz, in *Scanning Probe Microscopy: Electrical and Electromechanical Phenomena at the Nanoscale*, edited by S. Kalinin and A. Gruverman (Springer, New York, 2007), Vol. 1, pp. 215–253.
[8]C. Gao and X.-D. Xiang, Rev. Sci. Instrum. **69**, 3846 (1998).
[9]V. V. Talanov, A. Scherz, R. L. Moreland, and A. R. Schwartz, Appl. Phys. Lett. **88**, 134106 (2006).
[10]J. Kim, K. Lee, B. Friedman, and D. Cha, Appl. Phys. Lett. **83**, 1032 (2003).
[11]M. Tabib-Azar, D.-P. Su, and A. Pohar, Rev. Sci. Instrum. **70**, 1725 (1999).
[12]A. Imtiaz and S. M. Anlage, Ultramicroscopy **94**, 209 (2003).
[13]K. Fujimoto and Y. Cho, Jpn. J. Appl. Phys., Part 1 **43**, 2818 (2004).
[14]A. Imtiaz, S. M. Anlage, J. D. Barry, and J. Melngailis, Appl. Phys. Lett. **90**, 143106 (2007).
[15]J.-P. Bourgoin, M. B. Johnson, and B. Michel, Appl. Phys. Lett. **65**, 2045 (1994).
[16]A. Imtiaz and S. M. Anlage, J. Appl. Phys. **100**, 044304 (2006).
[17]M. D. Janezic, E. F. Kuester, and J.-B. Jarvis, IEEE MTT-S Int. Microwave Symp. Dig. **3**, 1817 (2004).
[18]*Handbook of Physics*, edited by W. Benenson, J. W. Harris, H. Stocker, and H. Lutz (Springer-Verlag, New York, 2002), p. 433.
[19]Ronold W. P. King, Margaret Owens, and Tai Tsun Wu, *Lateral Electromagnetic Waves: Theory and Application to Communications, Geophysical Exploration, and Remote Sensing* (Springer, New York, 1992).
[20]J. R. Wait, Radio Sci. **4**, 971 (1969).
[21]I. V. Lindell, E. Alanen, and K. Mannersalo, IEEE Trans. Antennas Propag. **AP-33**, 937 (1985).
[22]A. Tselev, S. M. Anlage, Z. Ma, and J. Melngailis, Rev. Sci. Instrum. **78**, 044701 (2007).
[23]D. M. Pozar, *Microwave Engineering*, 2nd ed. (Wiley, New York, 1998).